Geomechanics and Engineering, *Vol. 42, No. 4 (2025) 267-279*
https://doi.org/10.12989/gae.2025.42.4.267

Characterizing behavior of excavation-induced wall and ground movements with groundwater level and system stiffness

Qaisar Abbas[1a], Jonghyeog Yoon[2b], Donggun Nam[2c], Jiyeong Lee[2d] and Junhwan Lee*[2]

[1]*Interdisciplinary Research Center for Construction and Building Materials, King Fahd University of Petroleum and Minerals, 31261, Dhahran, Saudi Arabia*
[2]*School of Civil and Environmental Engineering, Yonsei University, 50, Yonsei-ro, Seodaemun-gu, Seoul 03722, Republic of Korea*

(*Received December 9, 2024, Revised July 21, 2025, Accepted July 24, 2025*)

Abstract. In this study, a design method using system stiffness influence factor (IF) was established to characterize the excavation-induced wall and ground movements with changes in groundwater level (GWL). The established factor for quantifying wall and ground behavior in this study considering GWL was regarded as an important aspect to prevent failures and ensure stable support systems design for the target structure. Irregular excavation configuration, common in urban areas, was considered using the three-dimensional finite element (FE) analysis, as well as different GWLs and various influence parameters for wall and support systems. Wall deflection and surface settlement were shown to decrease as the groundwater level was lowered and system stiffness was increased, especially with larger wall bending stiffness, higher wall embedment depth, and reduced vertical and horizontal strut spacings. These effects were particularly noted within re-entrant corner zones due to the corner stiffening effect. The influence of individual parameters was evaluated and quantified using the IF. A modification procedure for the IF was introduced to incorporate the effects of groundwater level, and the proposed method was shown to effectively predict wall deflection and ground settlement. Case example data confirmed the validity of this method, and its applicability in enhancing and optimizing excavation design was demonstrated. Overall, the proposed approach was offered as a practical and innovative framework for the design of excavation support systems under the influence of groundwater.

Keywords: finite element analysis; excavation; ground settlement; groundwater level; support system; wall deflection

1. Introduction

Rapid urbanization has led to an increasing demand for deep excavation projects necessary for the construction of high-rise buildings, basements, and underground infrastructures. A major concern for urban construction projects with deep excavation is the wall and ground movements induced by excavation. Stress release and changes in other mechanical state of soil from deep excavations can cause excessive lateral wall deflection and ground movement, potentially resulting in temporary or permanent damage to nearby facilities (Chen *et al*. 2023, Liu *et al*. 2023, Tabaroei and Chenari 2024, Abbas *et al.* 2024a, b). To ensure the stability and sustainability of urban construction, therefore, it is important to comprehend wall and ground movements behavior.

The extent of wall deformation and ground movements during excavation is influenced by various factors such as the stiffness of wall and support system, soil condition, groundwater level, excavation geometry, and construction processes (Ou *et al.* 1998, Wang *et al*. 2010, Goh *et al*. 2017). In particular, the stiffness of wall and support system is a crucial factor that affects wall and ground movements (Clough *et al*. 1989, Wang *et al.* 2010, Zhang *et al.* 2015, Giraldo et al. 2021). This stiffness is given by the structural stiffness condition, wall embedded depth, strut spacing, and geological conditions. Closely spaced struts, thicker walls, and deeper embedded depths all increase the system stiffness yet raise costs, thus requiring optimization (Ou *et al.* 1996, Finno *et al.* 2007, Zhang *et al*. 2019, Giraldo *et al*. 2021, Ling *et al.* 2024).

Many urban areas are located near rivers, and excavations in urban areas often take place below the groundwater table leading that the groundwater level during construction is crucial consideration to prevent possible accidents and ensure safety (Pujades and Jurado 2021). Wall and support systems offer essential resistance in excavation against exerted earth pressure and water pressure, while dewatering wells facilitate dry excavation conditions (Calin *et al*. 2017). Instances of excavation failure have been reported primarily due to high groundwater level and wrongly overestimated stability or the instability of the designed support system (Hsieh *et al*. 2008, Pong *et al*. 2012). This clearly indicates that designing a wall and support system with proper consideration of groundwater level variations is essential.

The impact of support-system stiffness on excavation has been frequently characterized using the system stiffness parameters proposed by Clough *et al*. (1989) and Bryson and Zapata-Medina (2012), and Abbas *et al*. (2024a). These parameters were adopted for the estimation of wall

*Corresponding author, Professor
E-mail: junlee@yonsei.ac.kr
[a]Ph.D.
[b]Ph.D. Student
[c]Ph.D. Student
[d]Ph.D.

ISSN: 2005-307X (Print), 2092-6219 (Online)

deflection, whereas the effect of groundwater level and its interaction with excavation and wall configurations were not specifically considered. The groundwater level can vary during excavation depending on the waterproof condition of installed wall, affecting the magnitude of wall deflection. For irregularly shaped excavations featuring re-entrant corners, wall deformation and ground deformations occur unsymmetrically (Abbas *et al.* 2023, 2024a, Sun *et al.* 2022), which would be further complicated with groundwater level. All these highlight the need for additional investigation and quantification of these effects.

In this study, the effect of groundwater level and support system stiffness on the wall and ground behavior are characterized, considering an irregular excavation configuration common in urban areas. The system stiffness influence factor was adopted to quantify the effect of groundwater level in interaction to support system stiffness. A design methodology using the stiffness influence factor considering the groundwater level is proposed. For this purpose, a series of 3D finite-element (FE) analyses were performed considering various groundwater level and support configurations and wall properties and analyzed.

2. Wall and ground movement behavior with excavation

2.1 Description of wall deflection and surface settlement

Analytical and empirical methods were employed to investigate wall and ground movements induced by excavation, with field monitoring data and numerical modelling results being utilized. Typical configurations of excavation-related movements are illustrated in Fig. 1, highlighting lateral wall deflection (δ_w), ground surface settlement (s_v), the depth to maximum wall deflection (z_m), and the influence zone of maximum surface settlement (d_m). It is specified by the common design criteria for wall serviceability limit state that the maximum wall deflection ($\delta_{w,m}$) should fall between 0.2% and 2% of the excavation depth (H_{ex}) (Clough and O'Rourke 1990, Long 2001, Bahrami *et al*. 2018).

The magnitude of $\delta_{w,m}$ and the depth to $\delta_{w,m}$ (i.e., z_m in Fig. 1) is usually proportional to H_{ex}, given as the following relationship

$$\delta_{w,m} = k_\delta H_{ex} \tag{1}$$

$$z_m = k_z H_{ex} \tag{2}$$

where k_δ and k_z = proportional coefficients for $\delta_{w,m}$ and z_m. The values of k_δ and k_z vary in the ranges of 0.1% to 1.5% and 0.5 to 1.4, respectively (Ou *et al*. 1998, Wang *et al.* 2010).

Ground settlement (s_v) behind the excavation wall is considered a critical design factor to avoid damage to adjacent structures. A triangular-shaped influence zone for the s_v profile behind the wall, extending to two and three times the excavation depth (H_{ex}) for sand and stiff clay, respectively, and a trapezoidal s_v profile was characterized for excavations in soft to medium clay (Clough and O'Rourke 1990). Hsieh and Ou (1998) reported that the maximum ground settlement ($s_{v,m}$) occurred at a distance of 0.5 times H_{ex} behind the wall (i.e., d_m in Fig. 1), with s_v at the wall being approximately 0.5 times $s_{v,m}$. The relationship between $s_{v,m}$ and $\delta_{w,m}$ is expressed as being proportional to each other, represented by the following relationship

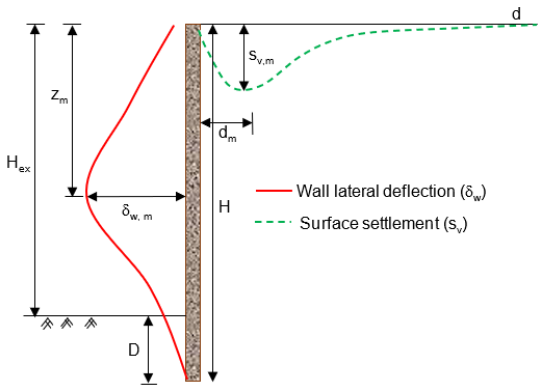

Fig. 1 Typical configurations describing wall and ground movements for excavation

$$s_{v,m} = \alpha \delta_{w,m} \tag{3}$$

where α = proportional coefficient. The values of α range from 0.4 to 1.5 for soft to medium soft clays and 0.1 to 0.7 for sand and stiff clays (Clough and O'Rourke 1990, Hsieh and Ou 1998, Leung and Ng 2007, Wang *et al*. 2010). These were proposed for regular excavation shape, and no detailed guidance on α has been presented for irregular cases, where the 3D excavation effect prevails, and changes in the groundwater level behind the wall.

2.2 Effect of support system stiffness

Clough *et al*. (1989) indicated that the wall movements are primarily caused by the excavation process and the installation of the supporting system. They introduced a design procedure for selecting appropriate support-system stiffness by presenting a chart that allows for the estimation of $\delta_{w,m}$ as a function of the stiffness influence factor (SIF), defined as follows

$$SIF = \frac{EI}{\gamma_w SP_V^4} \tag{4}$$

where EI = wall bending stiffness (E = elastic modulus of wall and I = moment of inertia of wall); SP_v = average vertical strut spacing; and γ_w = unit weight of water.

Bryson and Zapata-Medina (2012) noted that the SIF proposed by Clough *et al*. (1989) does not accurately represent the true nature of wall deformations in deep excavations due to its simplified assumptions regarding the influence parameters. As an alternative, they suggested a new SIF that incorporates soil-structure interaction, support and wall elements, and excavation stability, defined as follows

$$SIF = \frac{E_s}{E} \cdot \frac{SP_h SP_v H}{I} \cdot \frac{\gamma_s H_{ex}}{s_u} \tag{5}$$

where E_s and E = elastic moduli of soil and wall, respectively; I = moment of inertia of wall; SP_h and SP_v = horizontal and vertical spacings of strut, respectively; H = wall height; H_{ex} = excavation depth; γ_s = unit weight of soil; s_u = undrained shear strength of soil at the bottom of the excavation. Subsequently, similar charts and equations for SIF were proposed with modifications to Eqs. (4) and (5) (Moormann 2004, Zhang *et al*. 2015, Goh *et al.* 2017, Mu *et al.* 2021).

Abbas *et al*. (2024a) introduced a unified stiffness influence factor (I_F) that considers various components affecting excavation, including excavation configuration, soil type, support configuration, and wall stiffness. The I_F proposed by Abbas et al. (2024a) takes into account the actual excavation configuration, wall embedded depth, and strut properties to more accurately reflect field excavation conditions, represented by the following functional expression

$$I_F = \frac{E_s}{p_A} \cdot \frac{E}{p_A} \cdot \frac{IA_s}{SP_h SP_v A_i} \cdot \frac{D}{H_{ex}} \quad (6)$$

where E_s and E = elastic moduli of soil and wall; I = 2nd moment of inertia of wall; A_s = cross-sectional area of strut; H_{ex} = excavation depth; D = wall embedment depth; SP_h and SP_v = horizontal and vertical strut spacings; A_i = excavation influence area; and p_A = reference pressure equal to 100 kPa. I_F was then correlated to $\delta_{w,m}/H_{ex}$ given by (Abbas *et al*. 2024a)

$$\frac{\delta_{w,m}}{H_{ex}}(\%) = 0.2 \times I_F^{(-0.39)} \quad (7)$$

All the relationships of the wall influence factors presented so far pertained to a specific groundwater level (GWL) condition and are not applicable to the cases with generally observed conditions of GWL that varies frequently in periodic pattern depending on field and seasonal conditions. This clearly implies that further analyzing and accounting for variations in GWL for the wall behavior with excavation is necessary and essential to ensure the stability of the wall during excavation and for the design.

3. Numerical simulation of staged excavation

3.1 Description of finite element model

To characterize and quantify the impact of groundwater level on wall and ground behavior, the stiffness influence factor for excavation was analyzed considering various groundwater levels and stiffness conditions of wall and supports as well as strut configuration. For this purpose, a three-dimensional (3D) finite element (FE) analysis was conducted using PLAXIS 3D (PLAXIS 2020). In the numerical simulation, the actual excavation process of staged construction was included, incorporating changes in the factors influencing stiffness.

Fig. 2(a) shows the cross-sectional and plan views of the excavation configuration considered in the analysis. The excavation depth (H_{ex}) and the wall embedment depth (D) were set to 17 m and 13 m, respectively, reflecting typical urban excavation conditions (Zhang *et al*. 2019, Hsieh *et al*. 2019). A square-shaped re-entrant corner shape configuration was considered for excavation, with ratios W3/W4 = 1.0 and W3/W1 = 0.5, as shown in Fig. 2(b), where the widths of W1 and W3 were 60 m and 30 m, respectively. Support struts were placed in two directions, with horizontal spacing (SP_h) and vertical spacing (SP_v) of 5.0 m and 3.0 m, respectively. The diagonal struts were also placed at the corners of each excavation level.

Table 1 Values of embedment depth (D), strut spacing (SP_V, SP_h) and wall thickness (t) in FE analyses

D (m)	SP_h (m)	SP_v (m)	t (m)
6, 10, 13, 18	5	3	0.6
13	2.5, 5.0, 7.5, 10	3	0.6
13	5	1.5, 3.0, 5.1, 6.0	0.6
13	5	3.0	0.45, 0.69, 0.80 1.00, 1.20, 1.40

Fig. 2(c) indicates the locations of measuring points, selected as representative locations for each wall: P1-1 and P1-2 along W1 in longer and shorter strut zones, and P3 at the center of W3. For considering and analyzing the stiffness of wall and support system, various conditions of wall embedment depth (D), strut horizontal spacing (SP_h), strut vertical spacing (SP_v), and wall bending stiffness (EI) were prepared and adopted in the analysis, as summarized in Table 1. Note that the variations in wall bending stiffness (EI) were achieved by altering wall thickness (t) with a constant elastic modulus (E) of 24.82 GPa. Each case for the support system stiffness parameters in Table 1 were analyzed for three different groundwater levels: at the top surface (GL-0 m), at the mid-excavation level (GL-8.5 m), and at the base of the excavation depth (GL-17 m).

Fig. 3 illustrates the typical finite element (FE) model for the excavation configuration used in this study. The dimensions of the FE model were 230 m in length, 230 m in width, and 60 m in depth. The lateral boundaries were extended beyond the settlement influence zone to a distance of five times H_{ex} from the wall, in accordance with the recommendations of Hsieh and Ou (1998). Fixed conditions were applied along the bottom boundary of the model, while the lateral boundaries were constrained. The soil was represented using 10-noded tetrahedral continuum elements, with refined mesh arrangements near the wall where high stress levels were anticipated.

The wall was represented using eight-nodded quadrilateral plate elements, with an elastic modulus (E) of 24.82 GPa and a Poisson's ratio of 0.2. For the braced excavation, steel struts and walers were modeled as elastic beam elements, exhibiting axial stiffness (EA) values of 1.53 x 10^6 kN/m and 1.82 x 10^6 kN/m, respectively (Poh and Wong 1998, Zhang *et al*. 2015). The walers were designed to connect the wall and strut elements, mirroring their actual use in construction. Fixed connections were simulated for the structural support components (e.g., wall, struts, and walers), with the assumption that forces and moments are fully transferred. A strength reduction factor

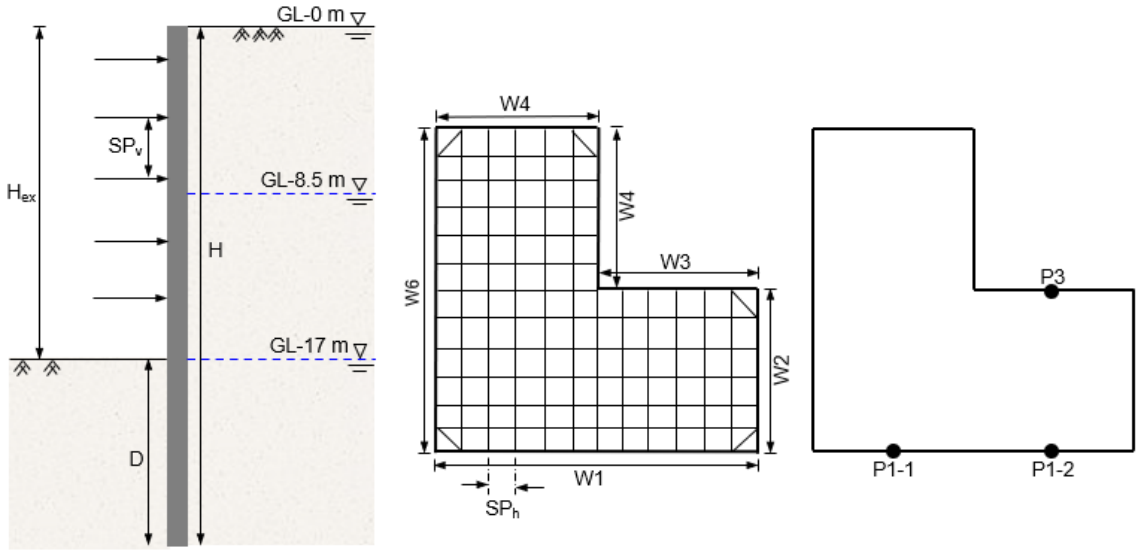

(a) Cross-sectional view (b) Plan view (c) Monitoring locations

Fig. 2 Cross-sectional view and monitoring locations considered in FE analysis model

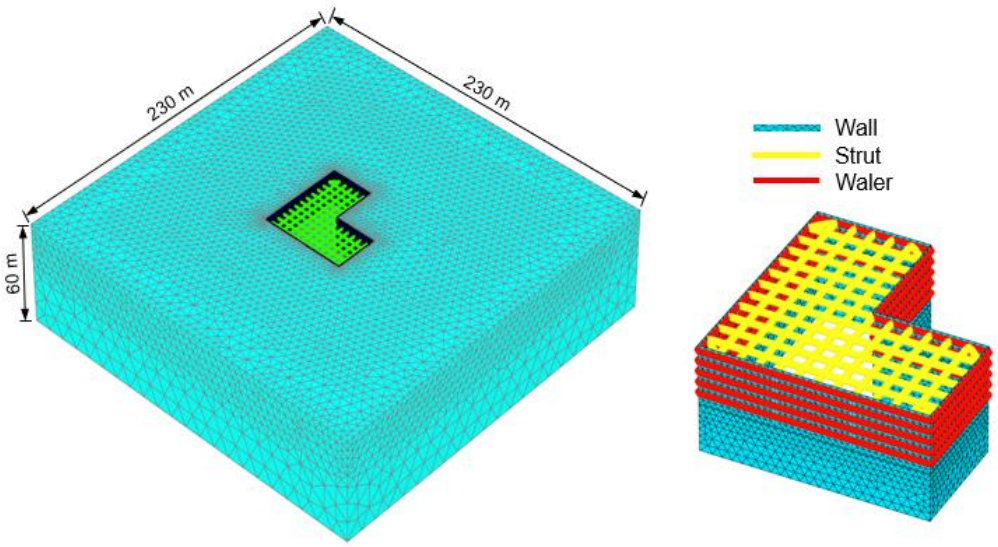

(a) Model description (b) Details of wall and supports

Fig. 3 Description of FE model: (a) Mesh configuration and (b) wall and strut system

(R_{int}) was applied to define the interface condition between the wall and soil, with a value of 0.7 assigned, considering excavation in sand (Zhang *et al*. 2019).

The soil constitutive behavior was represented using the advanced hardening soil small-strain (HSS) model, which effectively captures the non-linear elastoplastic response of the soil at small strains (Benz 2007, Benz *et al*. 2009). The HSS model is commonly employed in excavation-related modeling due to its suitability for simulating the unloading conditions of soil during excavation (Bryson and Zapata-Medina 2012, Zhang *et al*. 2015, Goh *et al*. 2017, Choosrithong and Schweiger 2020). The primary parameters of the HSS model include four reference stiffnesses: secant modulus (E_{50}), unloading-reloading modulus (E_{ur}), small-strain shear modulus (G_0), and oedometric modulus (E_{oed}). Other necessary parameters comprise the internal friction angle (ϕ'), cohesion intercept (c_{ref}), a power for stress-dependent stiffness formulation (m), and the failure ratio (R_f). In this study, sandy soil was utilized and modeled as a drained material. The typical properties of both dry and saturated sandy soil were derived from the literature (Goh *et al.* 2017, Zhang *et al.* 2019) and summarized in Table 2.

For model analysis, the initial geostatic stress state in the ground prior to excavation was established using the at-rest lateral earth pressure ratio (K_0). The final excavation depth of H_{ex} = 17 m was reached through a staged excavation process consisting of 12 stages, as shown in Fig. 4. Following the installation of the wall during the first stage, the soil was excavated to a depth of 2.0 m, where the

Table 2 Hardening soil small strain parameters used for FE analysis.

	γ (kN/m^3)	E_{50} (kN/m^2)	E_{oed} (kN/m^2)	E_{ur} (kN/m^2)	G_0 (kN/m^2)	$\gamma_{0.7}$ -	C_{ref} (kN/m^2)	ϕ' (°)	ν_{ur} -	K_0 -	R_f -
Sat. Sand	18.8	30,000	30,000	90,000	120,000	0.0002	0.05	35.4	0.3	0.42	0.90
Dry Sand	16.8	48,000	48,000	144,000	158,000	0.0002	0.05	37.8	0.3	0.38	0.93

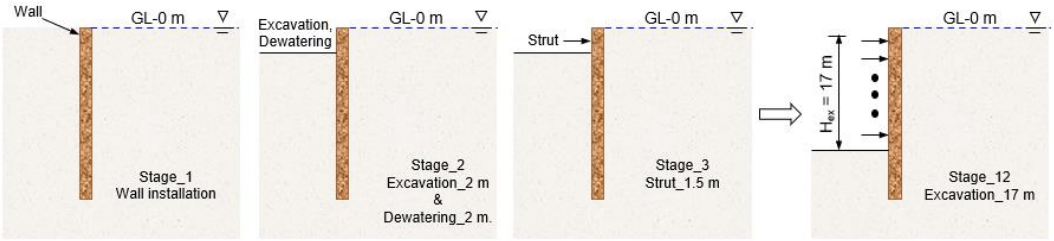

Fig. 4 Description of excavation process in FE analyses

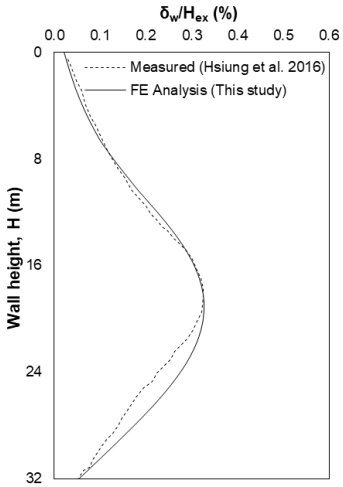

Fig. 5 Validation of FE model with measured wall deflection by Hsiung *et al*. (2016)

first level of supports (struts and walers) was installed at a depth of 1.5 m. This process was repeated until the excavation depth of H_{ex} = 17 m was attained, maintaining a vertical spacing of struts at 3.0 m. The final level of support was positioned at a depth of 13.5 m. The water level within of soil excavation, in accordance with the specified groundwater level conditions. In this study, a wished-in-place wall modeling approach was adopted without pre-excavation dewatering. Dewatering was simulated using the water level control method by adjusting groundwater levels inside and outside the excavation, consistent with recent studies (Zeng *et al.* 2021, 2022, Xue *et al*. 2024). However, significant wall movement may occur due to pre-excavation dewatering, as reported previously (Zeng *et al*. 2019, 2021, 2021, 2025). It should be noted that, like most numerical models, the FE analysis assumes idealized soil conditions and uniform material properties. Natural variability in soil stratigraphy and stiffness was not explicitly modeled, which may affect localized deformation patterns. Additionally, the wall-soil interface was simplified using a constant reduction factor, which may not fully capture the complex, stress-dependent interaction behavior under varying excavation stages.

To validate the finite element (FE) analyses performed in this study, field monitoring data from Hsiung *et al*. (2016) were used for comparison with the predicted results. The excavation was 20 m in length and 70 m in width, supported by a wall 0.9 m thick and 32 m deep. The final excavation depth was 16.8 m, with support provided by four levels of struts at a SP_h of 5.5 m. The subsurface conditions consisted primarily of loose to medium dense sand with thin interbedded clay layers. Soil properties for the numerical model were derived from in-situ DMT, CPT, and SPT correlations as reported in Hsiung *et al*. (2016).

Fig. 5 shows the measured and predicted lateral wall deflection (δ_w) profiles, with δ_w normalized by the final excavation depth (H_{ex}). The results indicated that the predicted profile closely matched the monitored data across the entire depth. In both cases, the maximum wall deflections were approximately 0.33% of H_{ex}, occurring at a depth of approximately 0.57H.

Minor deviations are attributed to idealizations in the model geometry, support configuration, and simplification of stratigraphy, which are common in FE analyses. Nonetheless, the validation confirms the model capability to replicate field performance trends in deep excavations. It should be noted that the influence of pre-existing underground structures on excavation behavior, through barrier effects, can either amplify or mitigate pit deformation depending on their geometry and stiffness. However, the practical validation case considered in this study did not account for such effects, but their significance has been highlighted in recent research (Yang *et al*. 2025, Zeng *et al*. 2022-2024, He *et al*. 2024, Xue *et al*. 2023).

4. Influence of groundwater level and stiffness parameters

4.1 Influence of groundwater level

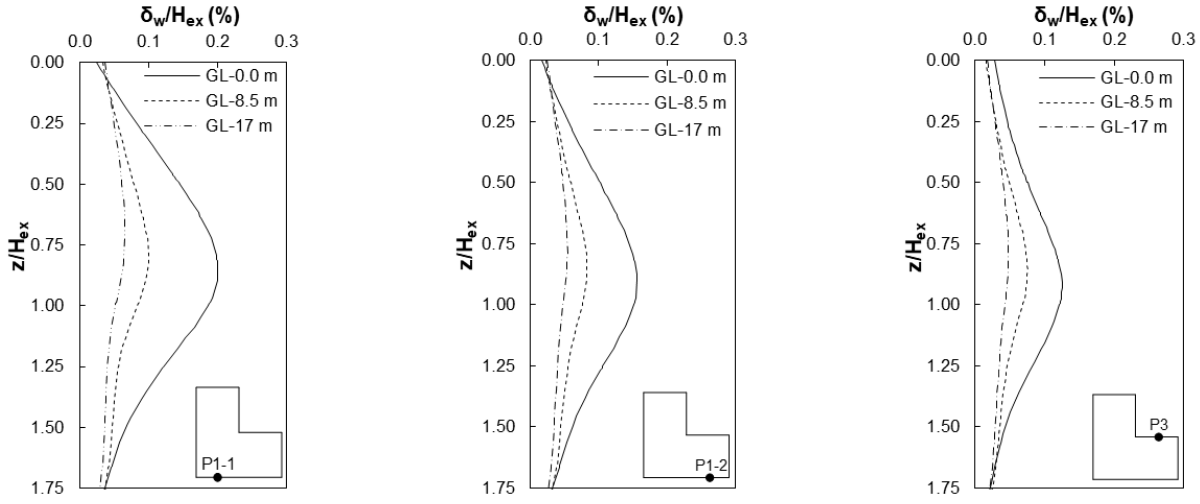

(a) P1-1 (b) P1-2 (c) P3

Fig. 6 Depth profiles of δ_w/H_{ex} for different groundwater levels at (a) P1-1, (b) P1-2 and (c) P3

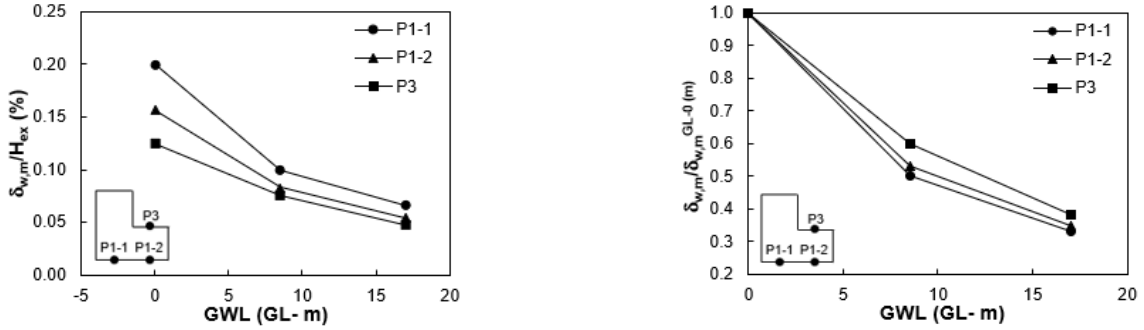

(a) $\delta_{w,m}/H_{ex}$ with GWL (b) $\delta_{w,m}/\delta_{w,m}^{GL\text{-}0\ (m)}$ with GWL

Fig. 7 Normalized maximum wall displacement with GWL for (a) $\delta_{w,m}/H_{ex}$ and (b) $\delta_{w,m}/\delta_{w,m}^{GL\text{-}0\ (m)}$

The depth profiles of normalized wall deflection (δ_w/H_{ex}) for the given excavation configuration in Fig. 2 were obtained from the FE analyses and plotted in Fig. 6. The results in Fig. 6 were those obtained for different groundwater levels (GWL) at P1-1, P1-2 and P3 locations [Fig. 2(c)] and plotted in Figs. 6(a)-6(c), respectively. The effect of GWL was clear and considerable, showing the magnitudes of changes that were variable depending on the location along the wall. The δ_w/H_{ex} profiles showed the typical bulging pattern with depth showing the maximum δ_w (i.e., $\delta_{w,m}$) at the depth of 13.6 m (i.e., $Z_m = 0.80H_{ex}$), which was consistent with other cases previously reported (Zhang *et al.* 2015, Hsiung *et al.* 2016). In all cases of Figs. 6(a)-6(c), the values of δ_w/H_{ex} decreased as GWL became deeper, and the smallest δ_w/H_{ex} profile was observed for GWL at the base of excavation depth (i.e., at GL-17 m). This was in agreement with results from centrifuge and field studies by Ou *et al.* 1993, Zeng *et al.* 2021, where wall deformations were shown to reduce under deeper GWL due to increases in effective stress and reduced hydraulic forces. It was also found that the values of δ_w/H_{ex} at P1-1 in Fig. 6(a) were largest, and those at P3 in Fig. 6(c) were smaller than for P1-2 in Fig. 6(b), due to the stiffening effect of re-entrant corner at P3. This corner stiffening effect was attributed to the three-dimensional geometric confinement, where intersecting walls and struts restrict wall deformation in both orthogonal directions. In addition, the proximity of the adjacent corner and shorter wall lengths further limit flexibility at P3, resulting in higher localized stiffness and lower wall deflection compared to other locations. These results exhibit the dependency of the GWL effect on the location along the wall, which needs to be properly considered in the design.

The values of $\delta_{w,m}/H_{ex}$ at P1-1, P1-2, and P3 were obtained from Fig. 6 and plotted with GWL (GL- m) in Fig. 7(a). $\delta_{w,m}/H_{ex}$ continuously decreased with lowering GWL from the ground surface to the base of the excavation depth. The values of $\delta_{w,m}$ in Fig. 7(a) were normalized with $\delta_{w,m}$ for the case of GWL at the ground surface (i.e., $\delta_{w,m}^{GL\text{-}0\ (m)}$) and plotted in Fig. 7(b). It was observed that P1-1 and P3 locations were more and less sensitive to the location of GWL, respectively. The low sensitivity of GWL at the P3 location stems from the three-dimensional excavation effect and stiffening effect on the re-entrant corner. P1-1 location was more sensitive to GWL as compared to P1-2 and P3 due to larger excavation influence area at P1-1, as compared P1-2 and P3.

The horizontal profiles of surface settlement (s_v/H_{ex}) behind the wall at P1-1, P1-2, and P3 were obtained and plotted in Fig. 8 for different locations of GWL. The s_v/H_{ex}

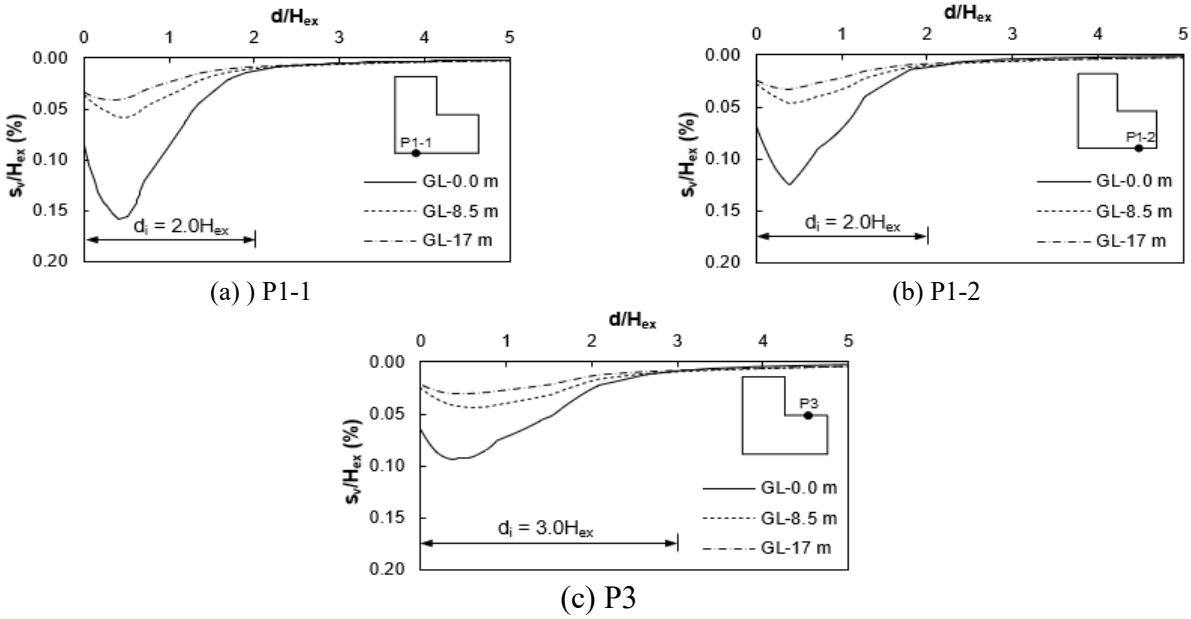

Fig. 8 Horizontal profiles of s_v/H_{ex} with groundwater level at (a) P1-1, (b) P1-2 and (c) P3

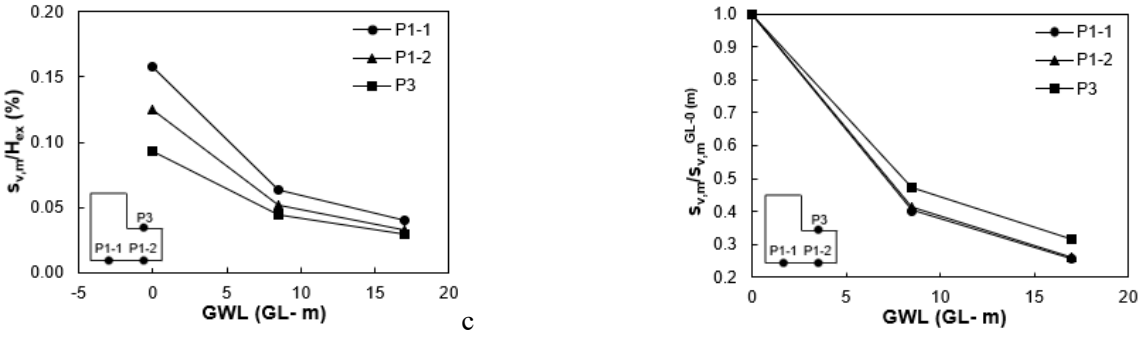

Fig. 9 Normalized maximum surface settlement with GWL for (a) $s_{v,m}/H_{ex}$ and (b) $s_{v,m}/s_{v,m}^{GL\text{-}0\ (m)}$

profiles showed the typical increasing-decreasing shape with distance from the wall. Similar to the results for δ_w/H_{ex} in Fig. 6, the values of s_v/H_{ex} decreased as GWL became deeper. The values of s_v/H_{ex} at P1-1 were largest whereas the influence zone of s_v/H_{ex} from the wall was wider for P3 as indicated in Fig. 8. This was because s_v/H_{ex} at P3 was affected by both sides of excavation with three dimensional effects at re-entrant corner of the excavation.

The values of the maximum s_v/H_{ex} ($s_{v,m}/H_{ex}$) were obtained from Fig. 8 and plotted with location of GWL in Fig. 9(a). Similar to the results for $\delta_{w,m}/H_{ex}$ in Fig. 7, $s_{v,m}/H_{ex}$ decreased with lowering GWL towards the base of the excavation depth. This relationship was consistent with the principles of soil-structure interaction, where inward wall deflection induced ground deformation and surface subsidence to satisfy equilibrium and compatibility. As supported by Clough and O'Rourke (1990) and Ou *et al.* (1993), the magnitude of surface settlement is commonly proportional to wall deflection, particularly in granular or lightly overconsolidated soils. From the normalized profiles of $s_{v,m}/s_{v,m}^{GL\text{-}0\ (m)}$ in Fig. 9(b), it was observed that the effect of GWL on $s_{v,m}$ was largest and smallest at P1-1 and P3, respectively. It was noted that the values of $s_{v,m}/H_{ex}$ directly related to the values of $\delta_{w,m}/H_{ex}$, however, the reduction of surface settlement with lowering GWL was more noticeable than for wall deflection in Fig. 7. The relatively greater reduction in $s_{v,m}/H_{ex}$ compared to $\delta_{w,m}/H_{ex}$ is attributed to the direct influence of GWL on effective stress changes and vertical deformation near the surface, especially in backfill zones.

4.2 Effect of stiffness influence parameters

The effects of various stiffness influence components, including wall stiffness (EI), embedment depth (D), and horizontal and vertical spacings of struts (SP_v, and SP_h), on $\delta_{w,m}/H_{ex}$ were analyzed for various locations of GWL and monitoring locations. Figs. 10(a)-10(c) show the effect of EI on $\delta_{w,m}/H_{ex}$ at P1-1, P1-2, and P3, respectively. The values of $\delta_{w,m}/H_{ex}$ decreased with increasing EI, more notably for GWL at ground surface (GL-0 m) and for lower values of EI at P1-1, P1-2 and P3 monitoring locations. The results in Fig. 10 indicate that EI plays a significant role in selecting support system stiffness, particularly for weak

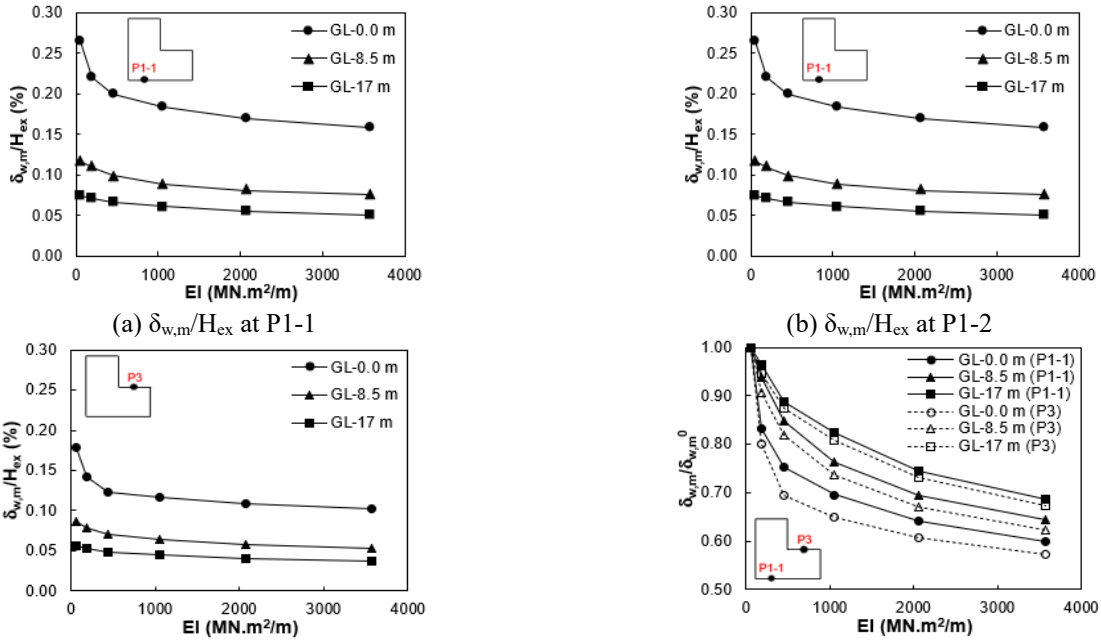

(a) $\delta_{w,m}/H_{ex}$ at P1-1 (b) $\delta_{w,m}/H_{ex}$ at P1-2

(c) $\delta_{w,m}/H_{ex}$ at P3 (d) $\delta_{w,m}/\delta_{w,m}^{0}$ at P1-1 and P3

Fig. 10 Values of $\delta_{w,m}/H_{ex}$ with EI for different GWL locations at (a) P1-1, (b) P1-2, (c) P3 and (d) $\delta_{w,m}/\delta_{w,m}^{0}$ at P1-1 and P3

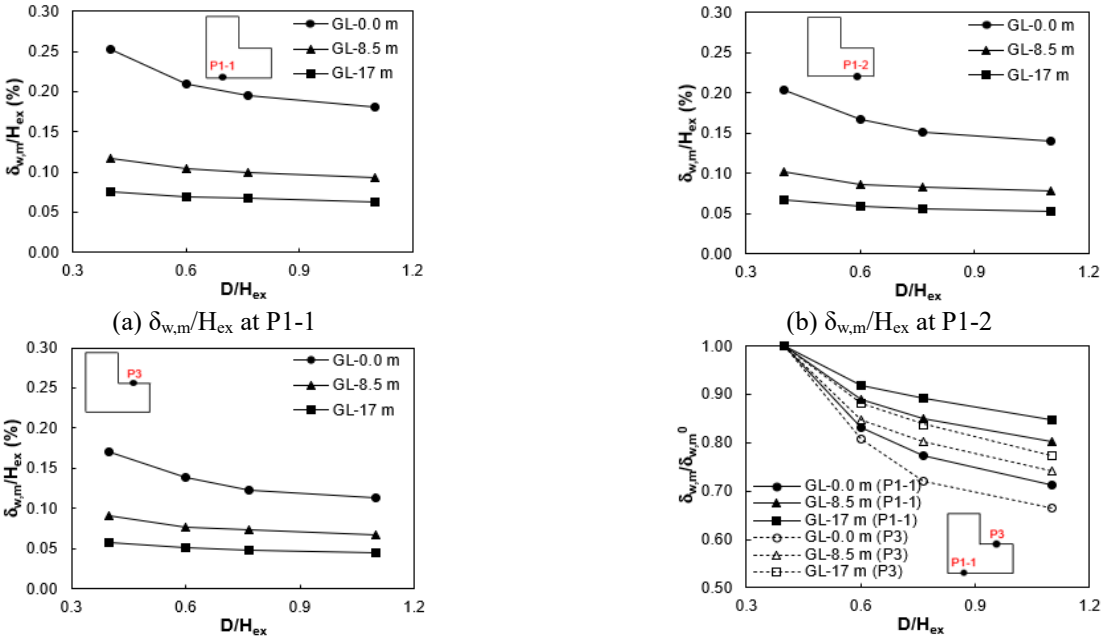

(a) $\delta_{w,m}/H_{ex}$ at P1-1 (b) $\delta_{w,m}/H_{ex}$ at P1-2

(c) $\delta_{w,m}/H_{ex}$ at P3 (d) $\delta_{w,m}/\delta_{w,m}^{0}$ at P1-1 and P3

Fig. 11 Values of $\delta_{w,m}/H_{ex}$ with D/H_{ex} for different GWL locations at (a) P1-1, (b) P1-2, (c) P3 and (d) $\delta_{w,m}/\delta_{w,m}^{0}$ at P1-1 and P3

ground with GWL at GL-0 m. Fig. 10(d) shows the normalized $\delta_{w,m}$ with those for the lowest EI (i.e., $\delta_{w,m}^{0}$). It was indicated that the effect of EI was larger at P3 than at P1-1 for all locations of GWL. These results aligned with previous parametric studies by Zeng *et al.* (2021), where greater EI was shown to significantly limit wall deformations in soft or granular soils. Although the values of $\delta_{w,m}/\delta_{w,m}^{0}$ at P1-2 were not plotted in Fig. 10(d), they were found to lie between those at the P1-1 and P3 monitoring locations for all GWL conditions.

Fig. 11 shows the values of $\delta_{w,m}/H_{ex}$ with D/H_{ex} for P1-1, P1-2, and P3 monitoring locations at different locations GWL. The values of $\delta_{w,m}/H_{ex}$ at P1-1, P1-2, and P3 decreased with increasing D/H_{ex}. The rate of $\delta_{w,m}/H_{ex}$ reduction was more noticeable at lower D/H_{ex}. From the normalized $\delta_{w,m}$ with those for the lowest D/H_{ex} (i.e., $\delta_{w,m}^{0}$)

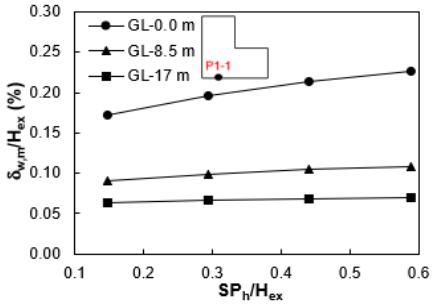

(a) $\delta_{w,m}/H_{ex}$ at P1-1

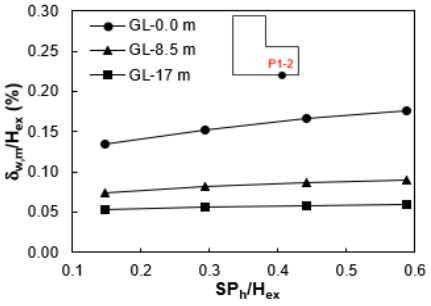

(b) $\delta_{w,m}/H_{ex}$ at P1-2

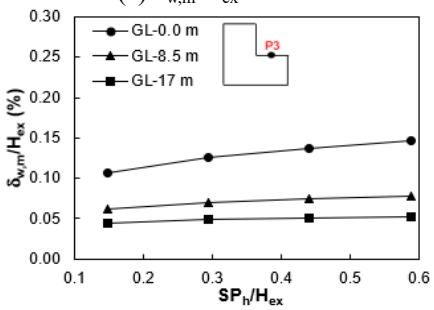

(c) $\delta_{w,m}/H_{ex}$ at P3

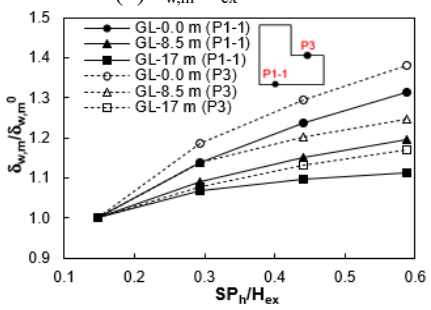

(d) $\delta_{w,m}/\delta_{w,m}^0$ at P1-1 and P3

Fig. 12 Values of $\delta_{w,m}/H_{ex}$ with SP_h/H_{ex} for different GWL locations at (a) P1-1, (b) P1-2, (c) P3 and (d) $\delta_{w,m}/\delta_{w,m}^0$ at P1-1 and P3

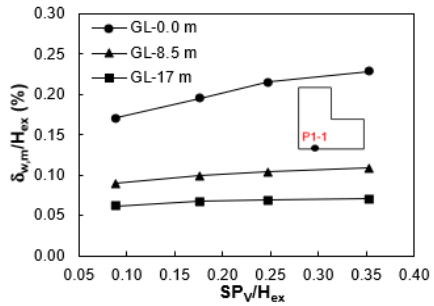

(a) $\delta_{w,m}/H_{ex}$ at P1-1

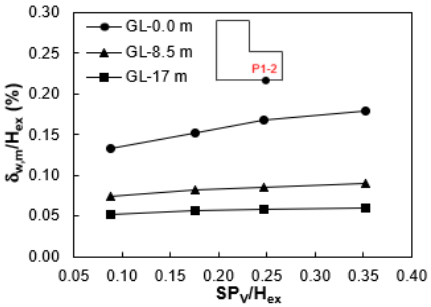

(b) $\delta_{w,m}/H_{ex}$ at P1-2

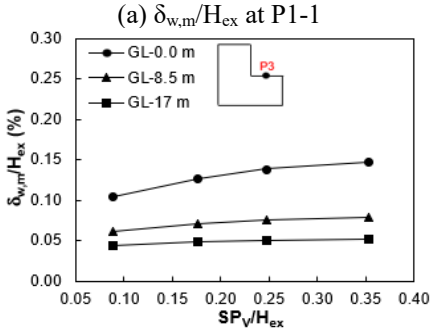

(c) $\delta_{w,m}/H_{ex}$ at P3

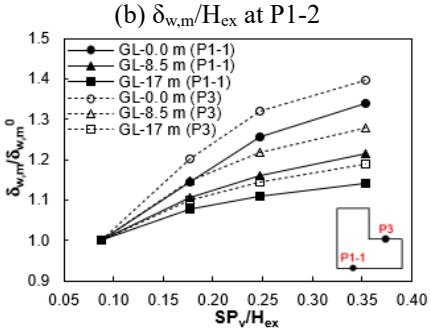

(d) $\delta_{w,m}/\delta_{w,m}^0$ at P1-1 and P3

Fig. 13 Values of $\delta_{w,m}/H_{ex}$ with SP_v/H_{ex} for different GWL locations at (a) P1-1, (b) P1-2, (c) P3 and (d) $\delta_{w,m}/\delta_{w,m}^0$ at P1-1 and P3

in Fig. 11(d), it was seen that the effect of D/H_{ex} was more pronounced and significant for higher GWL (i.e., GL-0) and at the P3 location, This indicated that the dry ground shows the minimum effect of wall embedment depths. This also highlighted the economic relevance and optimization for the determination of optimum support system parameters for excavation design.

Figs. 12 and 13 show the effects of SP_h and SP_v on $\delta_{w,m}$, where SP_h and SP_v were normalized with H_{ex}. The values of $\delta_{w,m}/H_{ex}$ increased with increasing SP_h/H_{ex} and SP_v/H_{ex} which was more pronounced for the higher GWL. Similar to the effect of EI in Fig. 10, the effects of SP_h and SP_v were more significant and beneficial for fully saturated soil conditions and P3. From Figs. 12 and 13, it was also found

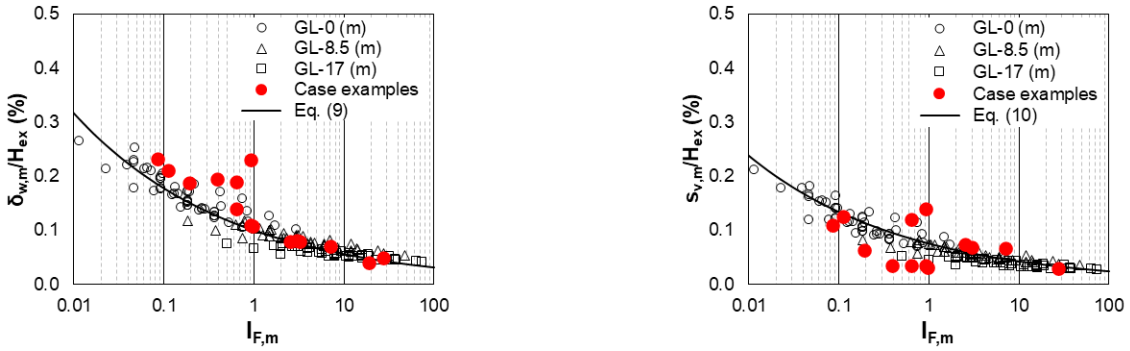

(a) $\delta_{w,m}/H_{ex}$ with $I_{F,m}$ (b) $s_{v,m}/H_{ex}$ with $I_{F,m}$

Fig. 14 Correlative relationships of (a) $\delta_{w,m}/H_{ex}$ and (b) $s_{v,m}/H_{ex}$ to $I_{F,m}$ with comparison using FE estimated and measured data from case examples

that SP_h and SP_v equally contributed to the support system stiffness, indicating the 3D nature of the strut effect, consistent with those reported by Clough and O'Rourke (1990). This confirms the need to consider both SP_v and SP_h for characterizing the support system stiffness.

5. Design consideration for groundwater level

The results and effects of groundwater level (GWL) obtained from this study were all characterized together in a unified design process. For this purpose, the system stiffness influence factor (I_F) given by Eq. (6) was adopted and modified considering the effect of GWL. Based on the influence tendency of GWL on $\delta_{w,m}/H_{ex}$ and $s_{v,m}/H_{ex}$ shown in Figs. 6 to 13, the effects of GWL locations and stiffness influence parameters were quantified and formulated by modifying the stiffness influence factor (I_F) of Eq. (6), given as follows

$$I_{F,m} = I_F \times (1 + \frac{GWL}{GWL_R}) \quad (8)$$

where $I_{F,m}$ = modified stiffness influence parameter; GWL = groundwater level and GWL_R = reference GWL depth = 1.0 m.

The values of $\delta_{w,m}/H_{ex}$ and $s_{v,m}/H_{ex}$ for all cases with various locations of GWL and stiffness parameters considered in this study were plotted as a function of $I_{F,m}$ in Figs. 14(a) and 14(b), respectively. From Fig. 14, while an approximately unified correlations were observed, it was seen that saturated ground condition with higher GWL and low support system stiffness showed a match to lower $I_{F,m}$ value than dry soil and stiffer support system. It was observed that the correlations of $\delta_{w,m}/H_{ex}$ and $s_{v,m}/H_{ex}$ to $I_{F,m}$ were both unique and consistent, showing decreasing tendencies with increasing $I_{F,m}$. From Figs. 14(a) and 14(b), the correlations of $\delta_{w,m}/H_{ex}$ and $s_{v,m}/H_{ex}$ with $I_{F,m}$ were obtained, given as follows

$$\frac{\delta_{w,m}}{H_{ex}}(\%) = 0.1 \times {I_{F,m}}^{(-0.25)} \quad (9)$$

$$\frac{s_{v,m}}{H_{ex}}(\%) = 0.075 \times {I_{F,m}}^{(-0.19)} \quad (10)$$

Case examples involving mixed soil conditions with various groundwater levels, excavation and support conditions were collected from the literature (Davies and Henkel 1980; Humpheson *et al*. 1986, Chu *et al*. 2001, Leung 2005, Houhou *et al*. 2019, Elbas *et al*. 2018, Hsiung *et al*. 2016) and adopted in comparison. It should be noted that the multi-stratum soil conditions were considered in the verifications using representative average stiffness values. This approach ensured validation of the proposed method under more realistic ground conditions. The values of $\delta_{w,m}/H_{ex}$, $s_{v,m}/H_{ex}$ and $I_{F,m}$ were obtained for each of the collected case examples and plotted in Figs. 14(a) and 14(b), where the proposed correlations of Eqs. (9) and (10) and the FE results were included. As shown in Fig. 14, the values of $\delta_{w,m}/H_{ex}$ and $s_{v,m}/H_{ex}$ from the case examples were found to be in reasonably close agreement with the proposed correlations of Eqs. (9) and (10). This indicates that the application of $I_{F,m}$ is effective for quantifying the combined influences of various stiffness parameters, GWL locations and inherent 3D characteristics for excavation and support system on wall and ground movements. Furthermore, it is also indicated that the proposed method enables a designer to select the appropriate support system stiffness based on limiting deformation for given location of GWL.

6. Conclusions

In this study, the influence of groundwater level (GWL) in relation to the stiffness of wall and support systems on wall and ground movements during excavation was investigated. A methodology was established to characterize the influence of GWL using the stiffness influence factor (I_F). A three-dimensional finite element analysis was performed considering various excavation configuration, GWLs and support system stiffness parameters. The following conclusions were drawn from the results:

1. The results for the irregular excavation showed that wall deflection (δ_w) and surface settlement (s_v) decreased as GWL deepened. The minimum values for δ_w and s_v were observed when GWL was at the base of

the excavation depth. Additionally, the values of δ_w and s_v were lower at the re-entrant corner at P3 compared to P1-1 and P1-2, which can be attributed to the corner stiffening effect of the re-entrant corner.

2. For the W1 wall, the location of maximum wall deflection (z_{max}) occurred at $0.8H_{ex}$ and shifted to a deeper depth for the re-entrant corner wall (W3) due to the three-dimensional effects. The influence zone of surface settlement (s_v) behind the wall was broader for the re-entrant corner wall, extending to $3.0H_{ex}$, compared to $2.0H_{ex}$ for W1, as ground behavior was affected by both sides of the excavation in the re-entrant corner zone.
3. For the system stiffness parameters, the values of $\delta_{w,m}$ decreased as overall stiffness increased, either by increasing EI and D or by reducing SP_v and SP_h. The effects of increasing system stiffness (EI, D, SP_v, and SP_h) for the stability of excavation were more significant for higher GWL and at the P3 location compared to P1-1.
4. The stiffness influence factor (I_F) was adopted and modified to quantify the effect of GWL location, which enabled effectively predicting wall and ground movement during excavation design. Case examples demonstrated that the modified stiffness factor ($I_{F,m}$) was effective and applicable for enhancing and optimizing excavation design.

Acknowledgments

This research was supported by the "National Research Foundation of Korea (NRF) grantfunded by the Korea government (MSIT) (Nos. RS-2024-00457308, RS-2025-00519983, and RS2025-24683148)".

References

Abbas, Q., Yoon, J. and Lee, J. (2023), "Characterization of wall deflection and ground settlement for irregular-shaped excavations with changes in corner configuration", *Int. J. Geomech.*, **23**(1), 04022258. https://doi.org/10.1061/(ASCE)GM.1943-5622.0002371.

Abbas, Q., Yoon, J. and Lee, J. (2024a), "A method for characterizing stiffness of a support system for excavation design", *Int. J. Geomech.*, **24**(2), 04023277. https://doi.org/10.1061/(ASCE)GM.1943-5622.0002591.

Abbas, Q., Yoon, J., Hahm, K. and Lee, J. (2024b), "Identifying failure connection area on wall for deep excavation based on system stiffness influence factor", *Eng. Fail. Anal.*, **164**, 108718. https://doi.org/10.1016/j.engfailanal.2023.108718.

Benz, T. (2007), "Small-strain stiffness of soils and its numerical consequences", Ph.D. thesis, Institute for Geotechnical Engineering, Univ. Stuttgart.

Benz, T., Vermeer, P.A. and Schwab, R. (2009), "A small-strain overlay model", *Int. J. Numer. Anal. Methods Geomech.*, **33**(1), 25-44. https://doi.org/10.1002/nag.702.

Bryson, L.S. and Zapata-Medina, D.G. (2012), "Method for estimating system stiffness for excavation support walls", *J. Geotech. Geoenviron. Eng.*, **138**(9), 1104-1115. https://doi.org/10.1061/(ASCE)GT.1943-5606.0000697.

Bahrami, M., Khodakarami, M.I. and Haddad, A. (2018), "3D numerical investigation of the effect of wall penetration depth on excavations behavior in sand", *Comput. Geotech.*, **98**, 82-92. https://doi.org/10.1016/j.compgeo.2018.02.003.

Clough, G.W., Smith, E.M. and Sweeney, B.P. (1989), "Movement control of excavation support system by iterative design", *Proc. ASCE Found. Eng.*, **2**, 869-884.

Clough, G.W. and O'Rourke, T.D. (1990), "Construction induced movements of in situ walls", *Proc. Des. Perf. Earth Retain. Struct. ASCE*, New York, 439-470.

Chu, R.P.K., Yau, P.K.F., Leung, D.H.K. and Mok, K.H. (2001), "Integrated approach for deep excavation along soft ground (MTRC) tunnels", *Proceedings of the 3rd Int. Conf. Soft Soil Eng.*, Hong Kong.

Calin, N., Cristian, R. and Ioan, B. (2017), "Dewatering system of a deep excavation in urban area-Bucharest case study", *Procedia Eng.*, **209**, 210-215. https://doi.org/10.1016/j.proeng.2017.11.038.

Choosrithong, K. and Schweiger, H.F. (2020), "Numerical investigation of sequential strut failure on performance of deep excavations in soft soil", *Int. J. Geomech.*, **20**(6), 04020063. https://doi.org/10.1061/(ASCE)GM.1943-5622.0001702.

Chen, W., Tang, L., Zhao, H., Yin, Q., Dong, S., Liu, J., Zhu, Z., and Ni, X. (2023), "Investigation of three-dimensional deformation mechanisms of existing tunnels due to nearby basement excavation in soft clay", *Geomech. Eng.*, **34**(2), 115-124. https://doi.org/10.12989/gae.2023.34.2.115.

Davies, R.V. and Henkel, D.J. (1980), "Geotechnical problems associated with the construction of Chater Station, Hong Kong", *Proceedings of the Conf. Mass Transp. Asia*, Mass Transit Railway Corporation, Hong Kong, Paper J3.

Elbaz, K., Shen, S.L., Tan, Y. and Cheng, W.C. (2018), "Investigation into performance of deep excavation in sand covered karst: A case report", *Soils Found.*, **58**, 1042-1058. https://doi.org/10.1016/j.sandf.2018.09.015.

Finno, R.J., Blackburn, J.T. and Roboski, J.F. (2007), "Three dimensional effects for support excavation in clay", *J. Geotech. Geoenviron. Eng.*, **133**(1), 30-36. https://doi.org/10.1061/(ASCE)1090-0241(2007)133:1(30).

Goh, A.T.C., Zhang, F., Zhang, W., Zhang, Y. and Liu, H. (2017), "A simple estimation model for 3D braced excavation wall deflection", *Comput. Geotech.*, **83**, 106-113. https://doi.org/10.1016/j.compgeo.2017.09.011.

Giraldo, J.R. and Bryson, L.S. (2021), "Excavation support system design method to limit damage in adjacent infrastructure", *J. Geotech. Geoenviron. Eng.*, **147**(12), 04021147. https://doi.org/10.1061/(ASCE)GT.1943-5606.0002696.

Humpheson, C., Fitzpatrick, A.J. and Anderson, J.M.D. (1986), "The basement and substructure for the new headquarters of the Hong Kong and Shanghai Banking Corporation, Hong Kong", *Proc. Institution of Civil Engineers*, **80**, 851-883.

Hsieh, P.G. and Ou, C.Y. (1998), "Shape of ground surface settlement profiles caused by excavation", *Can. Geotech. J.*, **35**(6), 1004-1017. https://doi.org/10.1139/t98-052.

Hsieh, P.G., Ou, C.Y. and Liu, H.T. (2008), "Basal heave analysis of excavations with consideration of anisotropic undrained strength of clay", *Can. Geotech. J.*, **45**(6), 788-799. https://doi.org/10.1139/T08-032.

Hsiung, B.C.B., Yang, K.H., Aila, W. and Hung, C. (2016), "Three-dimensional effects of a deep excavation on wall deflections in loose to medium dense sands", *Comput. Geotech.*, **80**, 138-151. https://doi.org/10.1016/j.compgeo.2016.06.011.

Hsieh, H.S., Wang, Z.Y., Lin, T.M. and Ge, L. (2019), "The system stiffness and wall displacement of a deep excavation strengthened with cross walls in soft clay", *J. GeoEng.*, **14**(4), 203-217. https://doi.org/10.6310/jgeo.201912_14(4).2.

Houhou, M. N., Emeriault, F. and Belounar, A. (2019), "Three-dimensional numerical back-analysis of a monitored deep

excavation retained by strutted diaphragm walls", *Tunn. Undergr. Sp. Tech.*, **83**, 153-164. https://doi.org/10.1016/j.tust.2018.09.018.

He, D., ZENG, C., Xu, C., Xue, X., Zhao, Y., Han, L. and Sun, H. (2024), "Barrier effect of existing building pile on the responses of groundwater and soil during foundation pit dewatering", *Water*, **16**(20), 2977. https://doi.org/10.3390/w16202977.

Long, M. (2001), "Database for retaining wall and ground movements due to deep excavations", *J. Geotech. Geoenviron. Eng.*, **127**(3), 203-224. https://doi.org/10.1061/(ASCE)1090-0241(2001)127:3(203).

Leung, H.Y. (2005), "The anisotropic small strain stiffness of completely decomposed tuff and its effects on deformations associated with excavations", Ph.D. thesis, The Hong Kong Univ. of Science and Technology, Hong Kong.

Leung, E.H.Y. and Ng, C.W.W. (2007), "Wall and ground movements associated with deep excavations supported by cast in situ wall in mixed ground conditions", *J. Geotech. Geoenviron. Eng.*, **133**(2), 129-143. https://doi.org/10.1061/(ASCE)1090-0241(2007)133:2(129).

Liu, M., Meng, F., Chen, R., Cheng, H. and Li, Z. (2023), "Numerical study on the lateral soil arching effect and associated tunnel responses behind braced excavation in clayey ground", *Transp. Geotech.*, **40**, 100970. https://doi.org/10.1016/j.trgeo.2023.100970.

Ling, T., Wu, X., Huang, F., Xia, J., Sun, Y. and Fenng, W. (2024), "Optimization of construction support scheme for foundation pits at zero distance to both sides of existing stations based on the pit corner effect", *Geomech. Eng.*, **38**(4), 381-395. https://doi.org/10.12989/gae.2024.38.4.381.

Moormann, C. (2004), "Analysis of wall and ground movements due to deep excavations in soft soil based on a new worldwide database", *Soils Found.*, **44**(1), 87-98. https://doi.org/10.3208/sandf.44.87.

Mu, L., Huang, M., Roodi, G.H. and Shi, Z. (2021), "Allowable wall deflection of braced excavation adjacent to pile-supported buildings", *Geomech. Eng.*, **26**(2), 161-173. https://doi.org/10.12989/gae.2021.26.2.161.

Ou, C.Y., Hsieh, P.G. and Chiou, D.C. (1993), "Characteristics of ground surface settlement during excavation", *Can. Geotech. J.*, **30**(5). https://doi.org/10.1139/t93-068.

Ou, C. Y., Chiou, D. C., and Wu, T.S. (1996), "Three-dimensional finite element analysis of deep excavations", *J. Geotech. Eng.*, **122**(5), 337-345. https://doi.org/10.1061/(ASCE)0733-9410(1996)122:5(337).

Ou, C.Y., Liao, J.T. and Lin, H. D. (1998), "Performance of diaphragm wall constructed using the top-down method", *J. Geotech. Geoenviron. Eng.*, **124**(9), 798-808. https://doi.org/10.1061/(ASCE)1090-0241(1998)124:9(798).

Poh, T.Y. and Wong, I.H. (1998), "Effects of construction of diaphragm wall panels on adjacent ground-field trial", *J. Geotech. Geoenviron. Eng.*, **124**(8), 749-756. https://doi.org/10.1061/(ASCE)1090-0241(1998)124:8(749).

Pong, K.F., Foo, S.L., Chinnaswamy, C.G., Ng, C.C.D. and Chow, W.L. (2012), "Design considerations for one-strut failure according to TR26-A practical approach for practicing engineers", *IES J. Part A: Civil Struct. Eng.*, **5**(3), 171-180. https://doi.org/10.1080/19373260.2012.709366.

PLAXIS (2020), PLAXIS 3D user manual, (Eds., Brinkgreve, R.B.J., Kumarswamy, S. and Swolfs, W.M.), Delft, Netherlands.

Pujades, E. and Jurado, A. (2021), "Groundwater-related aspects during the development of deep excavations below the water table: A short review", *Underground Space*, **6**, 35-45. https://doi.org/10.1016/j.undsp.2020.11.004.

Sun, Y., Che, Y., Gu, Z., Wang, R. and Fan, Y. (2022), "Measured structural response of a long irregular pit constructed using a top-down method", *Geomech. Eng.*, **31**(5), 489-503. https://doi.org/10.12989/gae.2022.31.5.489.

Tabaroei, A. and Chenari, R.J. (2024), "A simplified framework for estimation of deformation pattern in deep excavations", *Geomech. Eng.*, **37**(1), 31-48. https://doi.org/10.12989/gae.2024.37.1.031.

Wang, J.H., Xu, Z.H. and Wang, W.D. (2010), "Wall and ground movements due to deep excavations in Shanghai soft soils", *J. Geotech. Geoenviron. Eng.*, **136**(7), 985-994. https://doi.org/10.1061/(ASCE)GT.1943-5606.0000318.

Xue, T., Xue, X., Long, S., Chen, Q., Lu, S. and Zeng, C. (2023), "Effect of pre-existing underground structures on groundwater flow and strata movement induced by dewatering and excavation", *Water*, **15**(4), 814. https://doi.org/10.3390/w15040814.

Yang, K., Xu, C., Zeng, C., Zhu, L., Xue, X. and Han, L. (2025), "Analysis of recharge efficiency under barrier effects incurred by adjacent underground structures", *Water*, **17**(2), 257. https://doi.org/10.3390/w17020257.

Zhang, W., Goh, A.T.C. and Xuan, F. (2015), "A simple prediction model for wall deflection caused by braced excavation in clays", *Comput. Geotech.*, **63**, 67-72. https://doi.org/10.1016/j.compgeo.2014.10.003.

Zeng, C.F., Xue, X.L., Zheng, G., Xue, T.Y. and Mei, G.X. (2018), "Responses of retaining wall and surrounding ground to pre-excavation dewatering in an alternated multi-aquifer-aquitard system", *J. Hydro.*, **559**, 609-626. https://doi.org/10.1016/j.jhydrol.2018.02.069.

Zhang, W., Hou, Z., Goh, A. and Zhang, R. (2019), "Estimation of strut forces for braced excavation in granular soils from numerical analysis and case histories", *Comput. Geotech.*, **106**, 286-295. https://doi.org/10.1016/j.compgeo.2018.10.006.

Zeng, C.F., Zheng, G. and Xue, X.L. (2019), "Responses of deep soil layers to combined recharge in a leaky aquifer", *Eng. Geol.*, **260**, 105263. https://doi.org/10.1016/j.enggeo.2019.105263.

Zeng, C.F., Zheng, G., Zhou, X.F., Xue, X.L. and Zhou, H.Z. (2019), "Behaviours of wall and soil during pre-excavation dewatering under different foundation pit widths", *Comput. Geotech.*, **115**, 103169. https://doi.org/10.1016/j.compgeo.2019.103169.

Zeng, C.F., Xue, X.L. and Li, M.K. (2021), "Use of cross wall to restrict enclosure movement during dewatering inside a metro pit before soil excavation", *Tunn. Undergr. Sp. Tech.*, **112**, 103909. https://doi.org/10.1016/j.tust.2021.103909.

Zeng, C.F., Wang, S., Xue, X.L., Zheng, G. and Mei, G.X. (2021), "Evolution of deep ground settlement subject to groundwater drawdown during dewatering in a multi-layered aquifer-aquitard system: Insights from numerical modelling", *J. Hydro.*, **603**, 127078. https://doi.org/10.1016/j.jhydrol.2021.127078.

Zeng, C.F., Song, W.W., Xue, X.L., Li, M.K., Bai, N. and Mei, G.X. (2021), "Construction dewatering in a metro station incorporating buttress retaining wall to limit ground settlement: Insights from experimental modelling", *Tunn. Undergr. Sp. Tech.*, **116**, 104124. https://doi.org/10.1016/j.tust.2021.104124.

Zeng, C.F., Powrie, W., Xue, X.L., Li, M.K. and Mei, G.X. (2021), "Effectiveness of a buttress wall in reducing retaining wall movement during dewatering before bulk excavation", *Acta Geotechnica*, **16**, 3253-3267. https://doi.org/10.1007/s11440-021-01179-9.

Zeng, C.F., Liao, H., Xue, X.L., Long, S.C., Luo, G.J., Diao, Y. and Li, M.G. (2022), "Responses of groundwater and soil to dewatering considering the barrier effect of adjacent metro station on multi-aquifers", *J. Hydro.*, **612**, 128117. https://doi.org/10.1016/j.jhydrol.2022.128117.

Zeng, C.F., Wang, S., Xue, X.L., Zheng, G. and Mei, G.X. (2022), "Characteristics of ground settlement due to combined actions of groundwater drawdown and enclosure wall movement", *Acta Geotechnica*, **17**, 4095-4112. https://doi.org/10.1007/s11440-

022-01496-7.
Zeng, C.F., Chen, H.B., Liao, H., Xue, X.L., Chen, Q.N. and Diao, Y. (2023), "Behaviours of groundwater and strata during dewatering of large-scale excavations with a nearby underground barrier", *J. Hydro.*, **620**, 129400. https://doi.org/10.1016/j.jhydrol.2023.129400.
Zeng, C.F., Powrie, W., Chen, H.B., Wang, S., Diao, Y. and Xue, X.L. (2024), "Ground behavior due to dewatering inside a foundation pit considering the barrier effect of preexisting building piles on aquifer flow", *J. Geotech. Geoenviron. Eng.*, **150**(6). https://doi.org/10.1061/JGGEFK.GTENG-11978.
Xue, X.L., Sun, H.Y., Zeng, C.F., Chen, H.B., Zheng, G., Xu, C.J. and Han, L. (2024), "Why pile-supported building settled continuously after water level was stabilized during dewatering: Clues from interaction between pile and multi aquifers", *J. Hydro.*, **638**, 131539. https://doi.org/10.1016/j.jhydrol.2024.131539.
Zeng, C.F., Powrie, W., Xu, C.J. and Xue, X.L. (2025), "Wall movement during dewatering inside a diaphragm wall before soil excavation", *Underground Space*, **22**, 355-368. https://doi.org/10.1016/j.undsp.2025.01.003.

IC